Adhesion and Friction Properties of Polymer Brushes on Rough Surfaces: A Gradient Approach

ARTICLE *in* LANGMUIR · NOVEMBER 2013

Impact Factor: 4.46 · DOI: 10.1021/la402847z · Source: PubMed

5 AUTHORS, INCLUDING:

Shivaprakash Ramakrishna
ETH Zurich
15 PUBLICATIONS **66** CITATIONS
SEE PROFILE

Prathima Nalam
University of Pennsylvania
17 PUBLICATIONS **135** CITATIONS
SEE PROFILE

Nicholas D Spencer
ETH Zurich
403 PUBLICATIONS **11,606** CITATIONS
SEE PROFILE

Langmuir

Article

pubs.acs.org/Langmuir

Adhesion and Friction Properties of Polymer Brushes on Rough Surfaces: A Gradient Approach

Shivaprakash N. Ramakrishna, Rosa M. Espinosa-Marzal,[§] Vikrant V. Naik, Prathima C. Nalam,[†] and Nicholas D. Spencer*

Laboratory for Surface Science and Technology, Department of Materials, ETH Zurich, Wolfgang-Pauli-Strasse 10, 8093 Zurich, Switzerland

Supporting Information

ABSTRACT: The effect of nanoscale surface roughness on the lubrication properties of a polymer brush in a good solvent has been investigated. Friction and adhesion forces were measured by means of polyethylene colloidal-probe AFM across a 12 nm silica particle gradient before and after the adsorption of a poly(L-lysine)-*g*-poly(ethylene glycol) (PLL-*g*-PEG) polymer brush. The adsorption and conformation of the polymer chains were studied with multiple transmission and reflection infrared (MTR-IR) spectroscopy. The results show that prior to the adsorption of PLL-*g*-PEG on the gradient surface, the friction is high at the smooth end of the gradient while it decreases toward the rough end. Moreover, there is a direct correlation between friction and adhesion. Upon adsorption of the brushes, adhesion vanishes. In this case, a higher frictional force between the PEG-coated particle gradient substrate and the polyethylene sphere is observed at the rough end of the gradient in comparison to the smooth end. In spite of the increased adsorbed mass of PLL-*g*-PEG at the rough end of the gradient, theory and simulations show that the high curvature of the nanoparticles leads to a less swollen PEG brush in comparison to PEG brushes adsorbed on a planar surface, resulting in a lower repulsion, which can explain the observed increase in friction with particle density.

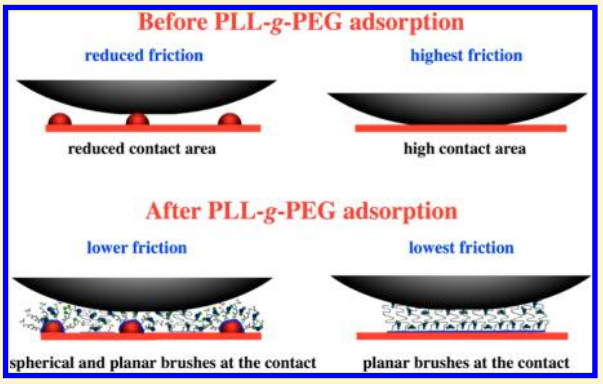

1. INTRODUCTION

Surface chemistry is known to play an important role in influencing tribological properties.[1,2] Chemical functionalization modifies the chemical state of the surface to create functional groups. Modifying the chemical composition of a surface by the incorporation of selected functional groups or polymer brushes has led to the ability to tailor the interfacial properties of surfaces according to requirements.[3−5]

Chemical modification by adsorption of molecularly thin organic layers can greatly alter the tribological behavior of micro/nanoscale devices. Self-assembled monolayers (SAMs) have been used to functionalize surfaces in MEMS/NEMS and can help to reduce the adhesion and friction forces between contacting parts.[6−9] On the other hand, polymer brushes, which are formed when polymer chains are tethered at one end to the substrate, while the other end freely dangles away from the surface, constrained only by its elasticity, can also present a high density of functional groups at interfaces that can be harnessed for various applications.[10−12] If strongly hydrated polymer-coated surfaces are compressed against each other, repulsive steric forces acting between the polymer brushes, osmotic and entropic in origin, maintain the surfaces separated, while preserving a high fluidity at the brush−brush interface and leading to very low friction coefficients.[13−15] If the distance between the grafted chains is smaller than the radius of the gyration; i.e., at high grafting densities, the chains maximize their steric forces, resulting in lubricious brush-like structures. However, at low grafting densities, polymer chains collapse to form mushroom-like structures, in good solvent, resulting in increased friction coefficients.

Polymer brushes have particularly attracted interest because of their efficiency at modifying the dynamic properties of surfaces under shear. They act as excellent boundary lubricants in the presence of good solvents.[16−18] The frictional and lubrication properties of polymer-coated surfaces constitute an important component in many areas of science and technology.[19,20]

Micromachined surfaces used in engineering and in MEMS/NEMS are stochastically rough on the nanometer scale. Surface roughness can play a crucial role in influencing the tribological properties of polymer-brush-coated surfaces, especially when the peak−valley variation is comparable to or exceeds the length of the brush. The topic should thus be critically examined.

There have been very few studies reported in the literature to examine the adhesion properties of polymer brushes tethered

Received: July 30, 2013
Revised: November 17, 2013
Published: November 22, 2013

to nanometer-scale rough surfaces under controlled conditions.[21,22] Here we attempt to understand the adhesion and friction properties of poly(L-lysine)-*graft*-poly(ethylene glycol) (PLL-*g*-PEG) copolymers (Figure 1), coated on a nanoparticle-

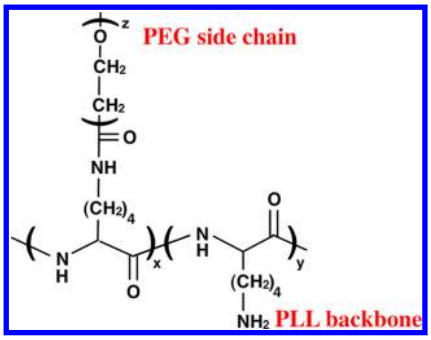

Figure 1. Molecular structure of a random copolymer of poly(L-lysine)-*graft*-poly(ethylene glycol) (PLL-*g*-PEG).

gradient surface. The PLL backbone is attracted electrostatically to negatively charged surfaces, such as many oxides at neutral pH, and the PEG side chains spontaneously form brush-like structures, which can effectively lubricate the oxide surfaces in an aqueous medium.[23]

A roughness gradient comprising gradually changing nanoparticle (12 nm in diameter) density along the length of the sample was prepared as described in ref 24. Adhesion and friction measurements, before and after the adsorption of PEG brushes, were carried out by means of colloidal-probe (polyethylene (PE)) microscopy. Multiple transmission and reflection (MTR) infrared spectroscopy was employed to investigate the adsorption of the polymer on the nanoparticle surface, and the effect of polymer conformation on the measured frictional response was discussed.

2. EXPERIMENTAL SECTION

The graft copolymer PLL(20 kDa)-*g*[3.5]-PEG(5 kDa) (PLL-*g*-PEG) was purchased from SuSoS AG (Dübendorf, Switzerland). The radius of gyration of the PEG chains (5 kDa) is taken as 2.82 nm (from ref 25). The monomer size $a \approx 3.58$ Å,[26] and the polymerization degree for 5 kDa PEG chains is $N \approx 110$. PLL-*g*-PEG adsorbs onto negatively charged substrates (in aqueous buffer) via the positively charged poly(L-lysine) backbone, forming brush-like structures. The brush configuration has been confirmed by numerical simulations for PLL(20)-*g*[3.5]-PEG brushes with a similar architecture.[27] From adsorption measurements,[28] the grafting density of the PEG brush on a smooth surface was determined to be $\sigma \sim 0.30 \pm 0.02$ chains per nm^2. As discussed for dextran brushes with similar architecture in ref 29, the influence of the PLL backbone on the brush conformation is negligible.

2.1. Gradient Surface. The silica nanoparticle density gradient sample was prepared by the immersion method.[24] A silicon wafer was cut to 2 cm × 1 cm and was marked along its length with a diamond cutter, at each millimeter. The wafer was then ultrasonicated twice for 20 min each in toluene, isopropanol, and water followed by plasma treatment for 2 min using an O_2 plasma cleaner (Harrick Scientific, Ithaca, NY). The oxidized silicon wafer was then rendered positively charged by adsorption of poly(ethylene imine) (Aldrich Chemicals) (PEI 0.5 mg/mL). The PEI-coated silicon wafer was mounted onto a linear-motion drive and was gradually immersed into a silica nanoparticle (diameter ≈ 12 nm) suspension (0.002 wt %) in deionized water. By slowly dipping the wafer into the suspension using a linear motion drive (Owis Staufen, Germany), i.e., by varying the immersion time of the silicon wafer in the nanoparticle suspension, a gradual variation of silica nanoparticle density along the length of wafer was obtained. Upon completion of the immersion process, the surface was flushed with a large amount of water while retrieving the sample in order to prevent further particle adsorption. The sample was then dried in a stream of nitrogen gas and immediately transferred to a furnace. The temperature inside the furnace was ramped to 1080 °C and held at this temperature for 2 h before it was cooled down to room temperature at a constant rate. This heating step not only burns away the PEI from the surface, but also the nanoparticles sinter to the SiO_2 on the wafer and firmly attach, thus becoming resistant to removal during subsequent adhesion and friction measurements. Topographical images were taken along the length of the sample by means of an atomic force microscope (Asylum AFM - MFP 3D, Santa Barbara, CA) using tapping mode at ambient conditions. A silicon cantilever (Olympus, Japan) with a resonant frequency of 300 kHz and a spring constant of around 26.1 N/m was used for imaging. The particle densities were obtained by averaging the counts from at least three images (Figure 2).

2.2. Adhesion and Friction Measurements. Adhesion and friction measurements were carried out on the 12 nm particle gradient sample by means of colloidal-probe AFM.[30] A polyethylene (PE)

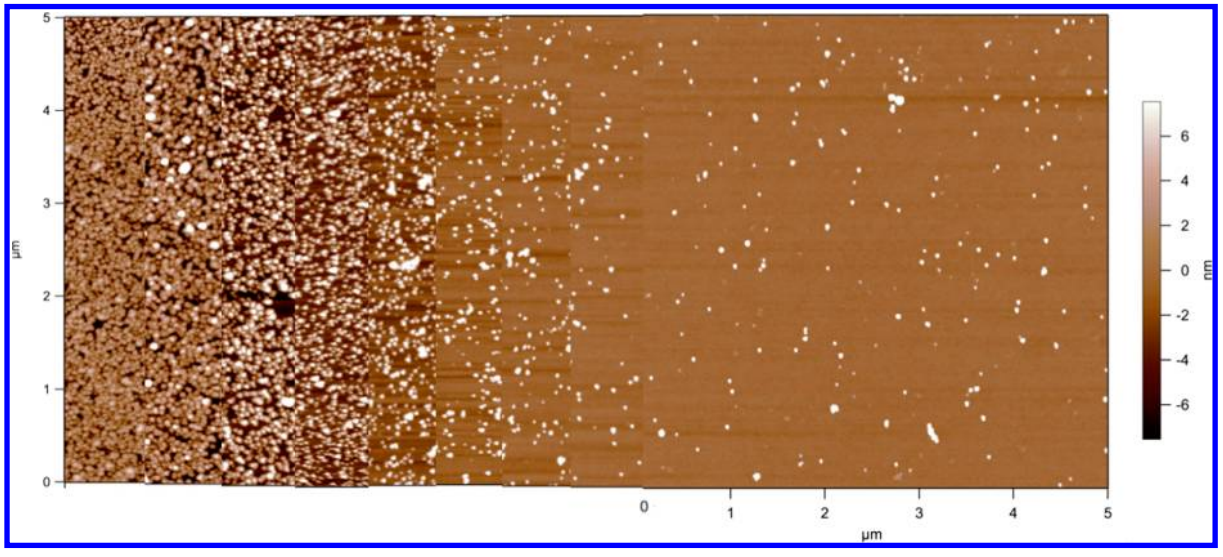

Figure 2. Overlapped AFM images (5 μm × 5 μm), taken along the length of the 12 nm particle roughness gradient sample. The height of the silica nanoparticles is obtained as 6 ± 2 nm.

dx.doi.org/10.1021/la402847z | *Langmuir* 2013, 29, 15251−15259

colloidal sphere (Type CL-2080, Kobo Products, Inc., South Plainfield, NJ) of radius ~9 μm was glued to a tipless cantilever (Mikromasch, Tallinn, Estonia) with normal spring constant (k_N) of 0.258 N/m and torsional spring constant (k_T) of 8.48×10^{-9} N·m. The normal spring constant was calculated by the thermal-noise method,[31] and torsional spring constant calibration was carried out according to Sader's method.[32] The lateral calibration was performed using the test-probe method, as described in detailed by Cannara et al.[33]

The measurements were carried out in HEPES (2-[4-(2-hydroxyethyl)piperazin-1-yl]ethanesulfonic acid, 10 mM) buffer at pH 7.4. Pull-off and friction forces were recorded at different particle densities along the length of the gradient sample, prior to polymer adsorption. The gradient sample was then immersed in a freshly prepared solution of PLL(20 kDa)-*g*(3.5)-PEG(5 kDa) (0.25 mg/mL in HEPES Buffer) for 40 min, washed with Milli-Q water, and dried with a stream of nitrogen gas. The adhesion and friction forces were recorded again (within the same area as before) along the length of the gradient sample after polymer adsorption. Around 100 pull-off measurements were mapped, and 10 friction loops were recorded at each particle density. Means and standard deviations of the measured adhesion and friction forces were calculated with Igor pro software (version 6.22A). The friction values are obtained by the averaged value of half of the subtracted individual trace values with its corresponding retrace values (trace−retrace/2) in a friction loop across the scan length. An average and standard deviation values obtained for ten such friction loops are reported (using the IGOR procedure file).

2.3. Multiple Transmission and Reflection Infrared Spectroscopy (MTR-IR). MTR-IR experiments[34] were performed on 36 × 18 mm^2 double-side-polished silicon wafers (0.5 mm ⟨111⟩, Si-Mat, Germany). 12 nm diameter silica nanoparticles were sintered on both sides of the wafers with the same procedure as described above, prior to the adsorption of PLL-*g*-PEG. Instead of a gradient, a substrate with a uniformly high particle density was prepared by immersing the entire wafer for 30 min in the silica nanoparticle suspension. MTR-IR experiments were performed on both PLL-*g*-PEG adsorbed on a smooth surface and on a particle-covered surface at the highest particle density.

MTR FTIR measurements were performed on a home-built MTR setup (Prof. Shoujun Xiao, University of Nanjing, China).[34,35] The double-side-polished Si wafer was placed between two gold mirrors, 2 mm apart such that its distance from the two mirrors was 0.3 and 1.2 mm and the simplified number of transmission passes was six. The spectra were acquired on a Bruker IFS66v FTIR spectrometer under vacuum with a resolution of 4 cm^{-1} using a mercury cadmium telluride (MCT) detector, cooled with liquid nitrogen. A bare Si wafer was used as background. Each experiment and background measurement consisted of 256 scans.

3. RESULTS

3.1. Adhesion Measurements with Varying Particle Density before and after PLL-*g*-PEG Adsorption. Figure 3 shows the measured adhesion force as a function of particle density (before and after PLL-*g*-PEG adsorption) along a 12 nm particle gradient under HEPES buffer. Similarly to previously obtained results on such gradient surfaces,[36,37] prior to the polymer adsorption (red squares), the adhesion at the rough end of the gradient (450 particles/μm^2) is lower than that measured at the smooth end. Upon decreasing the particle density, a slight decrease in the measured average adhesion force is observed due to the decrease in the real area of contact. Beyond a particle density of 210/μm^2, the PE colloid probe begins to come into contact with the substrate beneath, resulting in an increased adhesion force and standard deviation. The highest adhesion is observed at the smooth end (0 particles/μm^2). However, after adsorption of PLL-*g*-PEG, osmotic and steric forces lead to a repulsive force on the probe,[38] and negligible adhesion is measured at all particle densities along the gradient, as shown in Figure 3 (blue circles).

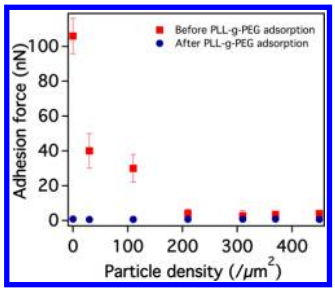

Figure 3. Measured adhesion forces as a function of particle density on a particle gradient under HEPES before (red) and after (blue) PLL-*g*-PEG adsorption. The cantilever has a normal spring constant of 0.258 N/m with a colloid sphere with radius = 9 μm. The approach and retract rate was held at 1 Hz over a vertical distance of 1 μm.

3.2. Friction Measurements on a Nanoparticle Gradient Sample before and after PLL-*g*-PEG Adsorption. Figure 4 shows the measured friction as a function of load for the 12 nm particle gradient (before (A) and after (B) PLL-*g*-PEG adsorption) in HEPES. The friction force was measured within the same area as where the adhesion force had been measured.

Similarly to the results obtained before,[37] the friction forces measured under HEPES are proportional to the real contact area and are influenced by the adhesion forces in the contact (Figure 4A). At the smooth end (0 particles/μm^2) of the gradient, the high contact area between the PE sphere and the silicon surface yields high adhesion and thus increases measured friction, whereas at the rough end (450 particles/μm^2) of the gradient, the decrease in the contact area results in reduced adhesion and hence also reduced friction. In contrast to previous observations on gradient substrates,[36,37] a reduction in particle density, down to a particle density of 210/μm^2, did not show a significant difference in the measured friction, although a slight decrease in the average friction is noticed at a particular load of 103 nN (see Figure 5). This, we believe, is due to the high spring constant of the cantilever used for these experiments, which cannot measure the small changes in friction forces at these particle densities. Below the particle density of 210/μm^2, the PE probe starts to touch the underneath substrate and the friction force increases due to the increased contact area. It should be noted that in the absence of polymer brushes the pressure acting on each nanoparticle present within the contact area increases with decreasing particle density along the gradient sample. The variation of the pressure and its distribution around the contact and the real area of contact between PE probe and the nanoparticles are discussed in detail in our previous paper.[37] It should also be noted that the increased contact pressures on each nanoparticle are not sufficient to result in plastic deformation of PE during our measurements. The yield strength of PE is reported to be close to 7 MPa.[37] A Hertzian calculation shows that plastic deformation can only potentially take place under conditions where the PE sphere is supported by a single nanoparticle, which does not occur for any of the explored particle densities. Also here, experiments are repeated several times with the same probe and sample with no noticeable change in the results being observed.

Upon adsorption of PLL-*g*-PEG (Figure 4B), the presence of repulsive steric forces and the absence of adhesion (or negligible adhesion forces that could be due to the hydro-

dx.doi.org/10.1021/la402847z | Langmuir 2013, 29, 15251−15259

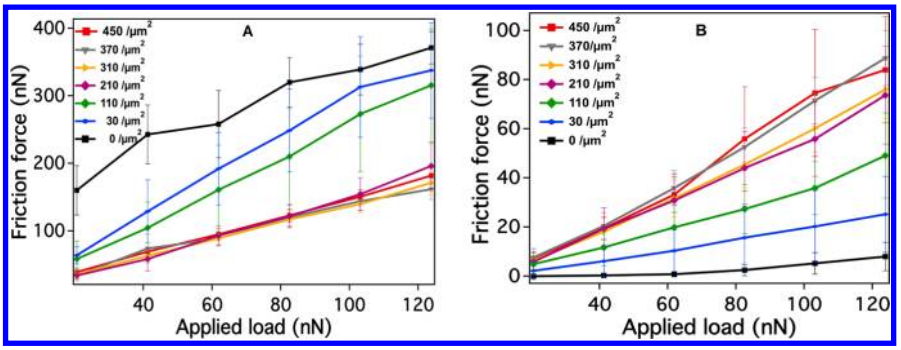

Figure 4. Measured friction vs load along the 12 nm nanoparticle gradient before (A) and after PLL-*g*-PEG adsorption (B) in HEPES. The normal and torsional spring constants of the cantilever were 0.258 N/m and 8.48 × 10^{-9} N·m, respectively. Radius of the PE sphere ≈9 μm. Note the difference in the *Y*-axes.

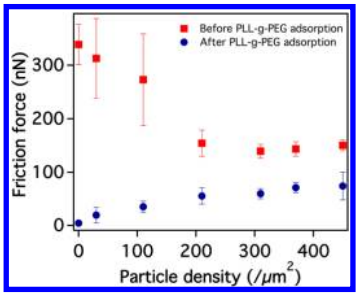

Figure 5. Measured friction forces across a gradient substrate before (red) and after (blue) PLL-*g*-PEG adsorption. The data points are extracted from Figure 4 at a normal load of 103 nN.

dynamic drag of the cantilever at the particular speed of measurement, see Figure S2 in Supporting Information) leads to the friction being dramatically decreased at the smooth end (0 particles/μm^2) in comparison to the rough end (450 particles/μm^2). With increasing particle density, the PEG-coated surfaces show an increase in the measured friction forces (Figure 5). However, the increase in the measured friction force at the highest particle densities (beyond 210 /μm^2) is less significant and is observed only at loads above 60 nN (Figure 4B). It should be noted that unlike in the case of a bare surface, the variation of pressure and the real area of contact following brush adsorption could not be calculated by using classical contact mechanics theories, in the absence of information concerning the elastic modulus of the polymer brushes absorbed on the nanoparticles.

Representative friction loops obtained at the smooth (0 particles/μm^2) and rough (450 particles/μm^2) ends of the gradient prior to and after polymer adsorption are shown in Figure 6. A dramatic decrease in the width of the friction loop is seen after the adsorption of PLL-*g*-PEG at the smooth end (see different *Y*-scales). However, at the rough end, the friction loops after adsorption of PLL-*g*-PEG show only a slight decrease in the width of the loop, indicating a reduced influence of PLL-*g*-PEG on the rough surface.

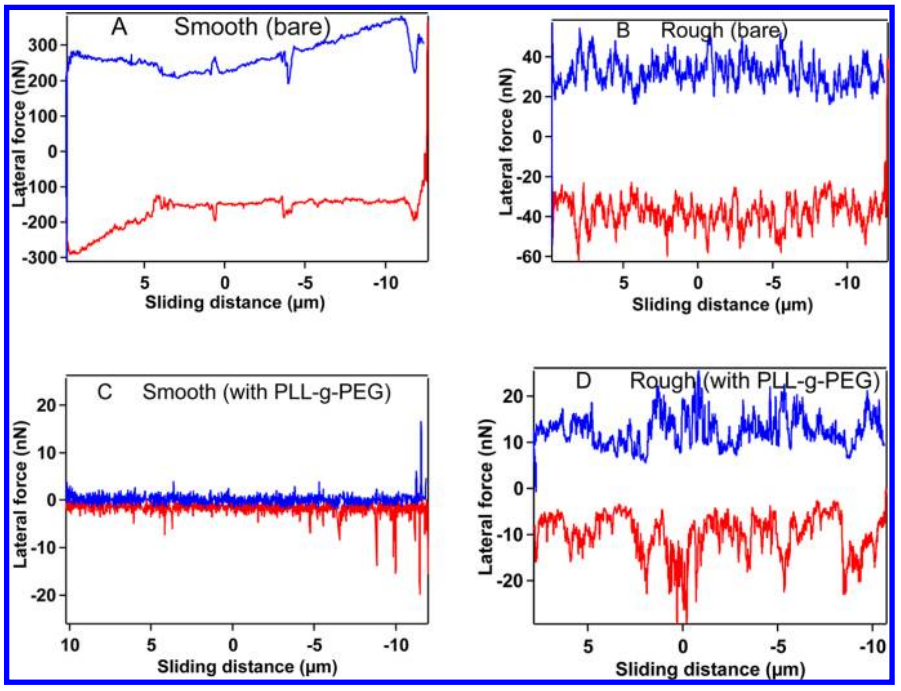

Figure 6. Friction loops obtained at a normal load of 40 nN at the smooth (0 particles/μm^2) and rough (450 particles/μm^2) ends of the gradient, before (A and B) and after (C and D) PLL-*g*-PEG adsorption. The scanning frequency of the friction loop was 1 Hz. Note the different scales for the *Y*-axes in the graphs.

dx.doi.org/10.1021/la402847z | *Langmuir* 2013, 29, 15251−15259

Figure 7 shows the friction loop obtained at low particle density (30 particles/μm^2) after the adsorption of PEG brushes.

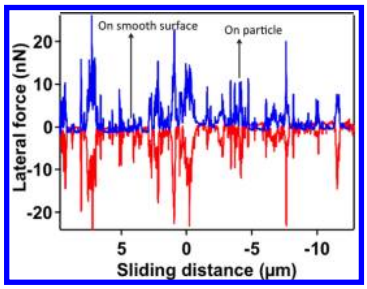

Figure 7. Friction loop obtained at low particle density (30 particles/μm^2) for an applied load of 40 nN, which shows a spike whenever the PE probe encounters the PEG chains tethered to the nanoparticles, whereas the loop shows low friction when the PE probe encounters PEG chains tethered to the flat surface. In order to account for the friction change with particle density and to include both on-particle and flat-surface effects, we averaged the friction force over the entire scan distance, thus representing the friction force relevant in a macroscopic experiment.

It is clearly seen in the friction loop that a step up (spike) occurs when the PE probe encounters the PEG-chain-covered particles, whereas the loop shows a drop in lateral force when the PE probe encounters the PEG-chain-covered smooth surface.

3.3. Adsorption and Conformational Study of PEG Brushes on Rough Surfaces Using Multiple Transmission−Reflection Spectrometry (MTR-IR). Understanding the adsorption and conformation of PLL-*g*-PEG on rough and smooth surfaces is important for understanding the observed friction and adhesion forces. Thus, in this study, a multiple transmission−reflection spectrometry (MTR-IR) was conducted to understand the conformation and orientation of PEG chains on the smooth and rough (particle) surfaces.

Figure 8 shows the MTR-IR spectra measured for PLL-*g*-PEG adsorbed on a 12 nm silica particle-covered surface (rough end, particle density of around 400/μm^2) and bare, smooth silica.

It is immediately clear from the IR peak intensities that the adsorption of PLL-*g*-PEG is higher on the particle-covered surface than on the smooth surface. Attention is focused on the CH_2 symmetric and asymmetric stretches of the PEG chain. While the CH_2 asymmetric stretch is observed at 2949 cm^{-1} for the smooth surface, it shifts to 2946 cm^{-1} on the particle surface. Similarly, the CH_2 symmetric stretch is observed at 2874 and 2871 cm^{-1} for smooth and particle-covered surfaces, respectively. The shift in the peak positions for symmetric and asymmetric stretches indicates different chemical environments, conformations, and packing of the chains. This in turn could be due to (a) effect of curvature on the conformations of the PEG chains, (b) a higher chain density of PLL-*g*-PEG on the particle surface, or (c) both. A distinction between these contributions is not possible.

It should be noted that prior to the MTR-IR experiments the samples were dried in air, and therefore some residual water could remain, particularly around the PEG chains. The MTR-IR experiments were performed under low vacuum conditions (0.1 mbar), and indeed, the presence of residual hydration water is evident by a broad band measured at ∼3200 cm^{-1}. Nevertheless, the brush conformation during the MTR-IR experiments is expected to differ from that in the buffer solution, which is a good solvent for PEG brushes:[26,39] in the MTR-IR experiments the PEG brushes are collapsed, while a swollen conformation can be expected in aqueous buffer on flat surfaces.[26,38] Theoretical and simulation studies have shown how the curvature of the surface influences the brush conformation of both swollen and collapsed brushes, which will be discussed and correlated with the results of the friction experiments in the next section.

4. DISCUSSION

The roughness of the substrate influences the friction force between the PEG-coated substrate and the PE colloidal sphere in aqueous buffer (Figure 5). MTR-IR measurement demonstrates a greater degree of polymer adsorption onto the rough substrate compared to the flat surface. Despite this, friction is higher at the rough end. The influence of the roughness on the friction must rely on the different conformation of the polymer brushes on flat and curved surfaces and its influence on the interaction forces. MTR-IR shows differences for the (partially) collapsed brushes on flat and rough surfaces. However, Wijmans and Zhulina[40] showed that the monomer density of the collapsed brushes in a bad solvent (air) is well described by a step profile, independently of the interface curvature, and this differs strongly from the swollen brush conformation in a good solvent. Therefore, it is not possible to infer accurate information about the different polymer conformation on flat or curved surfaces in a good solvent (HEPES buffer) from the MTR-IR results (under low vacuum) to explain the observed friction results.

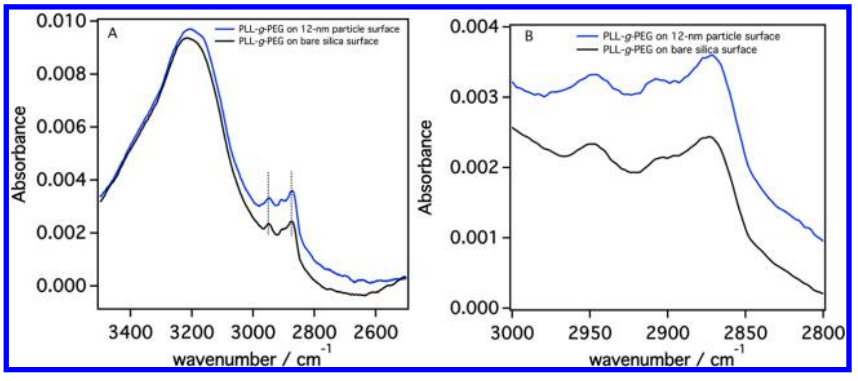

Figure 8. Zoomed regions of the MTR IR spectra showing (A) higher adsorption of PLL-*g*-PEG on the particle-covered surface. (B) CH_2 symmetric and asymmetric stretches of the PEG chain.

dx.doi.org/10.1021/la402847z | *Langmuir* 2013, 29, 15251−15259

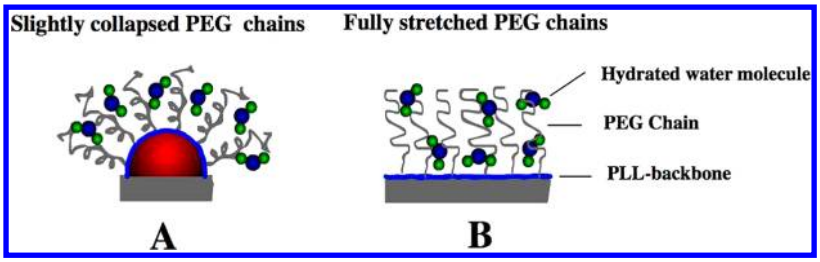

Figure 9. Schematic representation of the conformation of PLL-*g*-PEG on particle-covered (A) and smooth (B) surfaces.

Conformation and interaction forces of polymer brushes adsorbed onto curved surfaces have been studied theoretically[40−44] by means of numerical simulations[45,46] and experimentally.[47−49] The relevant parameter to distinguish the behavior of a planar brush from a brush adsorbed onto a curved surface is the ratio between the polymer brush height H and the radius of the central particle R_c. If this ratio is small (for short brushes or large radius of the spherical particle, i.e., small curvature), the monomers do not feel the curvature of the surface, so the system closely resembles a flat brush. On the other hand, if the ratio is sufficiently large, the available volume strongly increases in the radial direction, and the system begins to resemble a star polymer ($H \gg R_c$). In our experiments, this ratio H/R_c is ∼2, and therefore the effect of the spherical curvature on the PEG brush conformation is certainly relevant.[40]

Using straightforward geometrical arguments, the Alexander−de Gennes model[50,51] (or scaling theory) was extended by Daoud and Cotton to star-shaped polymers.[42] However, scaling theory is only a rough approximation to the real conformation of polymer brushes, since it assumes that all free chain ends are located at the outer region. A more sophisticated approach to the structure of grafted polymer layers at flat surfaces using self-consistent field (SCF) arguments is given in refs 52 and 53, based on Semenov's work on block copolymer melts. Wijmans and Zhulina[40] showed the effect of solvent quality on the conformation of brushes grafted to curved surfaces by using the SCF theory within the approximation of the mean-field model. They demonstrated that the chain ends are located throughout the whole brush with the exception of an exclusion zone in close proximity to the grafting surface. According to mean-field theory,[40] i.e., considering a parabolic profile for the monomer density, the maximum height of the PEG brushes adsorbed onto a flat surface H_{flat} in a very good solvent (where ν is a dimensionless virial coefficient that describes the solvent quality, assumed to be $\nu = 1$ for a good solvent) is given by

$$H_{flat} = \left(\frac{8}{\pi^2}\right)^{1/3} aN(\nu\sigma a^2)^{1/3} \quad (1)$$

which leads to a PLL-*g*-PEG brush height, H_{flat}, of 12.4 nm, with the values for N, a, and σ as given in the Experimental Section.

The average brush height on curved surfaces is obtained from the density profile at different solvent qualities within the mean-field approach. In a good solvent, a good agreement with the scaling law for star polymers is achieved for sufficiently long brushes,[40,45,46] i.e., if the dimensions of the nanoparticles are much smaller than the size of the chain. The scaling law gives

$$\frac{H_{sph}}{H_{flat}} \approx \left(\frac{H_{flat}}{R_c}\right)^{-2/5} \quad (2)$$

where H_{sph} is the average height of the spherical brush and R_c is the radius of the spherical particle, i.e., 6 nm. For the conditions of our experiment, $H_{sph} \approx 9.3$ nm, which demonstrates that PEG brushes are *less* stretched upon adsorption onto the nanoparticles with a diameter of 12 nm. This is just a rough estimation, since the selected PLL-*g*-PEG brushes are relatively short. However, the SCF theory[40] as well as molecular dynamics and density functional theory[45,46] predicts smaller thicknesses for spherical brushes than those predicted by eq 2 as well as that the monomer density goes from a power-like profile to a strong exponential decay in the outer region of the spherical brushes. All of these various approaches support the idea that the adsorption of PEG on the nanoparticles leads to a significantly less stretched polymer brush, as illustrated in Figure 9.

Interactions between brush-coated nanoparticles in a good solvent have been studied by MD simulations.[54] They show how the increase of the nanoparticle radius enhances both brush stretching and repulsion. Therefore, we can expect a smaller repulsion between the PEG brushes adsorbed onto the nanoparticles and the colloid sphere when compared to that between the equivalent planar PEG brushes and a colloidal sphere. For less-stretched brushes, higher friction can be expected, owing to the increased effective viscosity of the interfacial layer at each applied load.[55] Moreover, owing to the strong exponential decay in the monomer density of spherical brushes, it is to expect that curved polymer layers are more penetrable and therefore less repulsive upon initial overlap than flat layers at equal tethering density.[56] Thus, if the colloidal sphere interaction with the substrate is dominated by the interaction with the spherical brushes, higher friction can be expected, which accounts for the experimental results presented in Figures 4B and 5. Despite this, the adhesion between PEG brushes and the PE sphere was found to be negligible and not affected by roughness, since the presence of a swollen PEG brush on both flat and rough surfaces maintains an interfacial fluid at the contact, which prevents adhesion.

There could be also an issue that at higher loads the deformation of the PE sphere when compressed against PEG-coated nanoparticles would influence the measured friction forces. Thus, in order to exclude this effect, control measurements were conducted with colloidal-probe AFM on bare gradient surfaces against a PE colloid, immersed in buffer solution at high ionic strength (KNO_3, 200 mM, pH 7). At these high ionic strengths, the measured adhesion forces at both smooth (particle density $0/\mu m^2$) and rough ends (particle density $\sim 450/\mu m^2$) were found to be negligible. No significant difference was observed between the load-dependent friction

dx.doi.org/10.1021/la402847z | *Langmuir* 2013, 29, 15251−15259

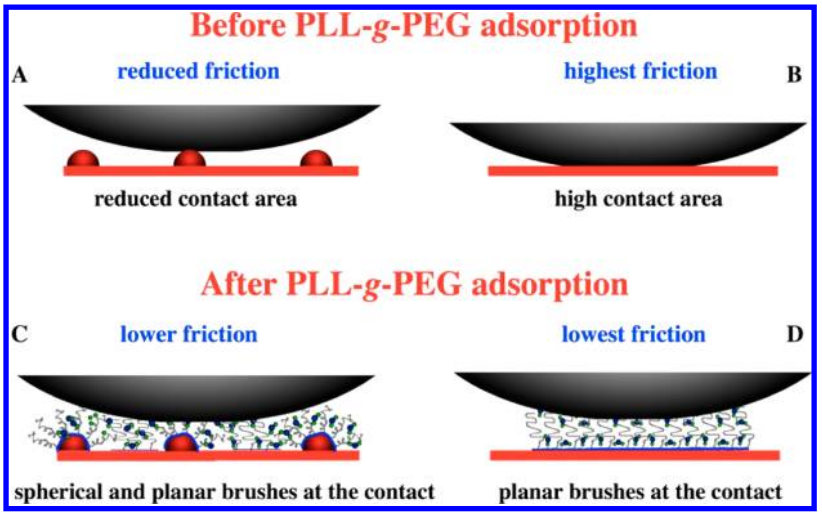

Figure 10. Schematics of the contact mechanics with and without PLL-*g*-PEG on rough (particle-covered) and smooth surfaces.

forces measured at the smooth and the rough end of gradient (S1), supporting the idea that the measured friction forces along the bare gradient are only determined by the adhesion force at the contact (Figure 4A). Accordingly, deformation of the PE sphere, if it would occur when compressed against a PEG-coated nanoparticle, does not appear to measurably affect the measured friction force. Thus, the change in friction along the PEG-coated nanoparticle gradient can be solely attributed to the conformational changes in the polymer-brush layer (Figure 4B).

The obtained adhesion and friction results on a particle-gradient substrate can be summarized by the schematic representation in Figure 10. On a smooth surface, in the absence of PEG brushes, the high contact area between the PE sphere and the silicon surface yields high adhesion and therefore the highest friction (Figure 10B). On the particle-covered surface (Figure 10A), the reduction in contact area due to the presence of nanoparticles decreases the adhesion and friction forces.

We observe two different regimes in the friction results of PEG-coated substrates. Upon adsorption of PLL-*g*-PEG onto the smooth surface (0 particles/μm^2) the lowest value of friction is achieved (Figure 10D). At particle densities smaller than 210 /μm^2, where the nanoparticles are very widely separated, the friction is affected by both planar and spherical brushes (Figure 10C). In this regime, friction increases with increasing particle density, as the influence of the spherical brushes increases. Above a critical particle density of 210 /μm^2, the PE colloid sphere (9 μm radius) does not sense the planar brush anymore, owing to the small distance between the nanoparticles. Thus, in this regime, friction is dominated by interaction with the spherical brushes.

5. CONCLUSION

A systematic study of the influence of nanoscale surface roughness on the tribological properties of PEG brushes using a nanoparticle density gradient substrate has been presented. The results show that in the absence of PEG brushes the friction is proportional to the real contact area and the measured adhesion force. Upon adsorption of PLL-*g*-PEG, adhesion vanishes, and the lowest friction is achieved on the smooth surface. At the rough end of the gradient surface, friction is higher due to the dominant interaction with the spherical PEG brushes. Spherical PEG brushes are less stretched than the same brushes adsorbed onto a flat surface, which leads to a smaller repulsion between the PEG brushes and the counter surface. Besides, the spherical brushes have a different monomer density leading to a more penetrable brush layer. Both effects result in an increase in the effective viscosity of the interfacial layer, which is responsible for the increase in friction. Upon decreasing the particle density on the surface, it becomes more likely that the PE probe will encounter the brushes adsorbed on the flat surface, which leads to a reduction of friction.

■ ASSOCIATED CONTENT

Ⓢ Supporting Information

S1: load-dependent friction forces for bare silicon surfaces across the particle gradient, at high ionic strengths, to estimate the contribution of PE sphere deformation on measured friction forces is discussed; S2: representative force−distance curves measured at the smooth and rough ends of the nanoparticle gradient substrate after PLL-*g*-PEG adsorption are discussed. This material is available free of charge via the Internet at http://pubs.acs.org.

■ AUTHOR INFORMATION

Corresponding Author

*E-mail nspencer@ethz.ch.

Present Addresses

[†]P.C.N.: Department of Mechanical Engineering and Applied Mechanics, University of Pennsylvania, 220 S. 33rd Street, Philadelphia, PA 19104.

[§]R.M.E.M: Environmental Engineering and Science, Civil and Environmental Engineering Department, University of Illinois at Urbana-Champaign, 3215 Newmark Laboratory, 205 N. Mathews Ave., Urbana, IL 61801.

Notes

The authors declare no competing financial interest.

■ ACKNOWLEDGMENTS

The authors acknowledge Dr. Venkataraman Nagaiyanallur and Dr. Lucio Isa from the Laboratory for Surface Science and Technology, Department of Materials, ETH Zurich, for fruitful discussions and their valuable suggestions.

REFERENCES

(1) Mori, S. Surface Chemistry in Tribology. *J. Jpn. Soc. Tribol.* **1997**, *42*, 683−688.

(2) McFadden, C.; Soto, C.; Spencer, N. D. Adsorption and Surface Chemistry in Tribology. *Tribol. Int.* **1997**, *30*, 881−888.

(3) Vahlberg, C.; Yazdi, G. R.; Petoral, R. M.; Syvaejaervi, M.; Uvdal, K.; Spetz, A. L.; Yakimova, R.; Khranovsky, V. Surface Engineering of Functional Materials for Biosensors. *IEEE Sens.* **2005**, 504−507.

(4) Mansur, A. A. P.; Do Nascimento, O. L.; Mansur, H. S. Enhancing Polymer-Modified Mortar Adhesion to Ceramic Tile Surface by Chemical Functionalization with Organosilanes. *Surf. Rev. Lett.* **2009**, *16*, 127−139.

(5) Bent, S. F.; Kachian, J. S.; Rodriguez-Reyes, J. C. F.; Teplyakov, A. V. Tuning the Reactivity of Semiconductor Surfaces by Functionalization with Amines of Different Basicity. *Proc. Natl. Acad. Sci. U. S. A.* **2011**, *108*, 956−960.

(6) Kim, B. J.; Kim, G. M.; Liebau, M.; Huskens, J.; Reinhoudt, D. N.; Brugger, J. "SAMs Meet MEMS": Surface Modification with Self-Assembled Monolayers for the Dry-Demolding of Photoplastic MEMS/NEMS. *Proc. - IEEE Micro Electro* **2001**, 106−109.

(7) Maboudian, R.; Ashurst, W. R.; Carraro, C. Self-Assembled Monolayers as Anti-Stiction Coatings for MEMS: Characteristics and Recent Developments. *Sens. Actuators, A* **2000**, *82*, 219−223.

(8) Rissanen, A.; Tappura, K.; Laamanen, M.; Puurunen, R.; Farm, E.; Ritala, M.; Leskela, M. Vapor-Phase Self-Assembled Monolayers for Improved MEMS Reliability. *IEEE Sens.* **2010**, 767−770.

(9) Bhushan, B.; Kasai, T.; Kulik, G.; Barbieri, L.; Hoffmann, P. AFM Study of Perfluoroalkylsilane and Alkylsilane Self-Assembled Monolayers for Anti-stiction in MEMS/NEMS. *Ultramicroscopy* **2005**, *105*, 176−188.

(10) Zobrist, C.; Sobocinski, J.; Lyskawa, J.; Fournier, D.; Miri, V.; Traisnel, M.; Jimenez, M.; Woisel, P. Functionalization of Titanium Surfaces with Polymer Brushes Prepared from a Biomimetic RAFT Agent. *Macromolecules* **2011**, *44*, 5883−5892.

(11) Choi, J.; Schattling, P.; Jochum, F. D.; Pyun, J.; Char, K.; Theato, P. Functionalization and Patterning of Reactive Polymer Brushes Based on Surface Reversible Addition and Fragmentation Chain Transfer Polymerization. *J. Polym. Sci., Polym. Chem.* **2012**, *50*, 4010−4018.

(12) Ayres, N. Polymer Brushes: Applications in Biomaterials and Nanotechnology. *Polym. Chem.* **2010**, *1*, 769−777.

(13) Klein, J.; Kumacheva, E.; Perahia, D.; Mahalu, D.; Warburg, S. Interfacial Sliding of Polymer-Bearing Surfaces. *Faraday Discuss.* **1994**, *98*, 173−188.

(14) Yan, X. P.; Perry, S. S.; Spencer, N. D.; Pasche, S.; De Paul, S. M.; Textor, M.; Lim, M. S. Reduction of Friction at Oxide Interfaces upon Polymer Adsorption from Aqueous Solutions. *Langmuir* **2004**, *20*, 423−428.

(15) Raviv, U.; Giasson, S.; Kampf, N.; Gohy, J. F.; Jerome, R.; Klein, J. Lubrication by Charged Polymers. *Nature* **2003**, *425*, 163−165.

(16) Klein, J.; Kamiyama, Y.; Yoshizawa, H.; Israelachvili, J. N.; Fredrickson, G. H.; Pincus, P.; Fetters, L. J. Lubrication Forces between Surfaces Bearing Polymer Brushes. *Macromolecules* **1993**, *26*, 5552−5560.

(17) Hartung, W.; Rossi, A.; Lee, S. W.; Spencer, N. D. Aqueous Lubrication of SiC and Si_3N_4 Ceramics Aided by a Brush-like Copolymer Additive, Poly(L-lysine)-graft-poly(ethylene glycol). *Tribol. Lett.* **2009**, *34*, 201−210.

(18) Nomura, A.; Ohno, K.; Fukuda, T.; Sato, T.; Tsujii, Y. Lubrication Mechanism of Concentrated Polymer Brushes in Solvents: Effect of Solvent Viscosity. *Polym. Chem.* **2012**, *3*, 148−153.

(19) Zhang, S. L.; Tsou, A. H.; Li, J. C. M. Scratching Behavior of Elastomeric Poly(dimethylsiloxane) Coatings. *J. Polym. Sci., Part B: Polym. Phys.* **2002**, *40*, 1530−1537.

(20) Hutchings, L. R.; Narrianen, A. P.; Thompson, R. L.; Clarke, N.; Ansari, L. Modifying and Managing the Surface Properties of Polymers. *Polym. Int.* **2008**, *57*, 163−170.

(21) Synytska, A.; Svetushkina, E.; Martina, D.; Bellmann, C.; Simon, F.; Ionov, L.; Stamm, M.; Creton, C. Intelligent Materials with Adaptive Adhesion Properties Based on Comb-like Polymer Brushes. *Langmuir* **2012**, *28*, 16444−16454.

(22) Svetushkina, E.; Puretskiy, N.; Ionov, L.; Stamm, M.; Synytska, A. A Comparative Study on Switchable Adhesion Between Thermoresponsive Polymer Brushes on Flat and Rough Surfaces. *Soft Matter* **2011**, *7*, 5691−5696.

(23) Lee, S.; Muller, M.; Ratoi-Salagean, M.; Voros, J.; Pasche, S.; De Paul, S. M.; Spikes, H. A.; Textor, M.; Spencer, N. D. Boundary Lubrication of Oxide Surfaces by Poly(L-lysine)-g-Poly(ethylene glycol) (PLL-g-PEG) in Aqueous Media. *Tribol. Lett.* **2003**, *15*, 231−239.

(24) Huwiler, C.; Kunzler, T. P.; Textor, M.; Voros, J.; Spencer, N. D. Functionalizable Nanomorphology Gradients via Colloidal Self-Assembly. *Langmuir* **2007**, *23*, 5929−5935.

(25) Perrino, C.; Lee, S.; Choi, S. W.; Maruyama, A.; Spencer, N. D. A Biomimetic Alternative to Poly(ethylene glycol) as an Antifouling Coating: Resistance to Nonspecific Protein Adsorption of Poly(L-lysine)-graft-dextran. *Langmuir* **2008**, *24*, 8850−8856.

(26) Nalam, P. C. *Polymer Brushes in Aqueous Solvent Mixtures*; ETH: Zurich, 2012.

(27) Feuz, L.; Leermakers, F. A. M.; Textor, M.; Borisov, O. Adsorption of Molecular Brushes with Polyelectrolyte Backbones onto Oppositely Charged Surfaces: A Self-Consistent Field Theory. *Langmuir* **2008**, *24*, 7232−7244.

(28) Nalam, P. C.; Daikhin, L.; Espinosa-Marzal, R. M.; Clasohm, J.; Urbakh, M.; Spencer, N. D. Two-Fluid Model for the Interpretation of Quartz Crystal Microbalance Response: Tuning Properties of Polymer Brushes with Solvent Mixtures. *J. Phys. Chem. C* **2013**, *117*, 4533−4543.

(29) Espinosa-Marzal, R. M.; Nalam, P. C.; Bolisetty, S.; Spencer, N. D. Impact of Solvation on Equilibrium Conformation of Polymer Brushes in Solvent Mixtures. *Soft Matter* **2013**, *9*, 4045−4057.

(30) Ducker, W. A.; Senden, T. J.; Pashley, R. M. Direct Measurement of Colloidal Forces Using an Atomic Force Microscope. *Nature* **1991**, *353*, 239−241.

(31) Butt, H. J.; Jaschke, M. Calculation of Thermal Noise in Atomic-Force Microscopy. *Nanotechnology* **1995**, *6*, 1−7.

(32) Green, C. P.; Lioe, H.; Cleveland, J. P.; Proksch, R.; Mulvaney, P.; Sader, J. E. Normal and Torsional Spring Constants of Atomic Force Microscope Cantilevers. *Rev. Sci. Instrum.* **2004**, *75*, 1988−1996.

(33) Cannara, R. J.; Eglin, M.; Carpick, R. W. Lateral Force Calibration in Atomic Force Microscopy: A New Lateral Force Calibration Method and General Guidelines for Optimization. *Rev. Sci. Instrum.* **2006**, *77*, 053701.

(34) Liu, H. B.; Venkataraman, N. V.; Bauert, T. E.; Textor, M.; Xiao, S. J. Multiple Transmission-Reflection Infrared Spectroscopy for High-Sensitivity Measurement of Molecular Monolayers on Silicon Surfaces. *J. Phys. Chem. A* **2008**, *112*, 12372−12377.

(35) Liu, H. B.; Venkataraman, N.; Spencer, N. D.; Textor, M.; Xiao, S. J. Structural Evolution of Self-Assembled Alkanephosphate Monolayers on TiO_2. *ChemPhysChem* **2008**, *9*, 1979−1981.

(36) Ramakrishna, S. N.; Clasohm, L. Y.; Rao, A.; Spencer, N. D. Controlling Adhesion Force by Means of Nanoscale Surface Roughness. *Langmuir* **2011**, *27*, 9972−9978.

(37) Ramakrishna, S. N.; Nalam, P. C.; Clasohm, L. Y.; Spencer, N. D. Study of Adhesion and Friction Properties on a Nanoparticle Gradient Surface: Transition from JKR to DMT Contact Mechanics. *Langmuir* **2013**, *29*, 175−182.

(38) Heuberger, M.; Drobek, T.; Spencer, N. D. Interaction Forces and Morphology of a Protein-Resistant Poly(ethylene glycol) Layer. *Biophys. J.* **2005**, *88*, 495−504.

(39) Muller, M. T.; Yan, X. P.; Lee, S. W.; Perry, S. S.; Spencer, N. D. Preferential Solvation and its Effect on the Lubrication Properties of a Surface-Bound, Brushlike Copolymer. *Macromolecules* **2005**, *38*, 3861−3866.

(40) Wijmans, C. M.; Zhulina, E. B. Polymer Brushes at Curved Surfaces. *Macromolecules* **1993**, *26*, 7214−7224.

(41) Semenov, A. N. Contribution to the Theory of Microphase Layering in Block-Copolymer Melts. *Zh. Eksp. Teor. Fiz.* **1985**, *88*, 1242−1256.
(42) Daoud, M.; Cotton, J. P. Star Shaped Polymers - A Model for the Conformation and Its Concentration-Dependence. *J. Phys. (Paris)* **1982**, *43*, 531−538.
(43) Halperin, A.; Tirrell, M.; Lodge, T. P. Tethered Chains in Polymer Microstructures. *Adv. Polym. Sci.* **1992**, *100*, 31−71.
(44) Szleifer, I.; Carignano, M. A. Tethered Polymer Layers. *Adv. Chem. Phys.* **1996**, *94*, 165−260.
(45) Binder, K.; Milchev, A. Polymer Brushes on Flat and Curved Surfaces: How Computer Simulations Can Help to Test Theories and to Interpret Experiments. *J. Polym. Sci., Part B: Polym. Phys.* **2012**, *50*, 1515−1555.
(46) Verso, F. L.; Egorov, S. A.; Milchev, A.; Binder, K. Spherical Polymer Brushes Under Good Solvent Conditions: Molecular Dynamics Results Compared to Density Functional Theory. *J. Chem. Phys.* **2010**, *133*, 184901.
(47) Savin, D. A.; Pyun, J.; Patterson, G. D.; Kowalewski, T.; Matyjaszewski, K. Synthesis and Characterization of Silica-graft-Polystyrene Hybrid Nanoparticles: Effect of Constraint on the Glass-Transition Temperature of Spherical Polymer Brushes. *J. Polym. Sci., Part B: Polym. Phys.* **2002**, *40*, 2667−2676.
(48) Ohno, K.; Morinaga, T.; Takeno, S.; Tsujii, Y.; Fukuda, T. Suspensions of Silica Particles Grafted with Concentrated Polymer Brush: Effects of Graft Chain Length on Brush Layer Thickness and Colloidal Crystallization. *Macromolecules* **2007**, *40*, 9143−9150.
(49) Dukes, D.; Li, Y.; Lewis, S.; Benicewicz, B.; Schadler, L.; Kumar, S. K. Conformational Transitions of Spherical Polymer Brushes: Synthesis, Characterization, and Theory. *Macromolecules* **2010**, *43*, 1564−1570.
(50) Alexander, S. Adsorption of Chain Molecules with a Polar Head a Scaling Description. *J. Phys. (Paris)* **1977**, *38*, 983−987.
(51) de Gennes, P. G. Conformations of Polymers Attached to an Interface. *Macromolecules* **1980**, *13*, 1069−1075.
(52) Milner, S. T.; Witten, T. A.; Cates, M. E. Theory of the Grafted Polymer Brush. *Macromolecules* **1988**, *21*, 2610−2619.
(53) Zhulina, E. B.; Borisov, O. V.; Priamitsyn, V. A. Theory of Steric Stabilization of Colloid Dispersions by Grafted Polymers. *J. Colloid Interface Sci.* **1990**, *137*, 495−511.
(54) Verso, F. L.; Yelash, L.; Egorov, S. A.; Binder, K. Interactions Between Polymer Brush-Coated Spherical Nanoparticles: The Good Solvent Case. *J. Chem. Phys.* **2011**, *135*, 214902.
(55) Klein, J. Shear, Friction, and Lubrication Forces Between Polymer-Bearing Surfaces. *Annu. Rev. Mater. Sci.* **1996**, *26*, 581−612.
(56) Halperin, A.; Kröger, M.; Zhulina, E. B. Colloid-Brush Interactions: The Effect of Solvent Quality. *Macromolecules* **2011**, *44*, 3622−3638.